Crystal Structures and Electronic Absorption Spectra of Two Modifications of $Cr(SeO_2OH)(Se_2O_5)$

M. Wildner*,[1] and M. Andrut†

*Institut für Mineralogie und Kristallographie, Geozentrum, Universität Wien, Althanstraße 14, A-1090 Wien, Austria; and
† GeoForschungsZentrum Potsdam, Telegrafenberg A3, D-14473 Potsdam, Germany

Single crystals of two modifications (I and II) of $Cr(SeO_2OH)$ (Se_2O_5) have been synthesized under low-hydrothermal conditions. Their structures have been investigated using single-crystal X-ray diffraction data up to $\sin\theta/\lambda = 0.76$ Å^{-1} [I: monoclinic, space group $P2_1/n$, $a = 7.517(2)$ Å, $b = 12.516(3)$ Å, $c = 7.381(2)$ Å, $\beta = 91.46(1)°$, $Z = 4$, $R1 = 0.030$ for 1562 $F_o >$ $4\sigma(F_o)$ and 114 variables; II: orthorhombic, space group $Pnma$, $a = 8.782(2)$ Å, $b = 11.172(3)$ Å, $c = 7.545(2)$ Å, $Z = 4$, $R1 =$ 0.031 for 752 $F_o > 4\sigma(F_o)$ and 65 variables]. In $Cr(SeO_2OH)$ (Se_2O_5)-I, sheets—built up from isolated CrO_6 octahedra and Se_2O_5 groups—are linked via the SeO_2OH groups and rather strong hydrogen bonds. This structure is isotypic with the corresponding compounds of Mn(III) and Fe(III). $Cr(SeO_2OH)$ (Se_2O_5)-II represents a new framework structure type, also composed of isolated CrO_6 octahedra and Se_2O_5 and SeO_2OH groups, but with very weak hydrogen bonds. The hydrogen-bonding schemes of both compounds were further investigated by FTIR microscope spectrometry in the range 7000–1000 cm^{-1}, yielding a typical AB-band spectrum for phase I. Furthermore, polarized electronic absorption spectra were measured in the range 33,000–12,500 cm^{-1} using UV–VIS microscope spectrometric techniques. According to the weak distortions of the CrO_6 octahedra in both compounds, the observed band splittings and polarization effects are rather weak. Hence, crystal field calculations were performed assuming O_h symmetry, resulting in the following crystal field parameter sets; I, $Dq = 1558$, $B_{35} = 653$, $B_{55} = 760$, $C = 2920$ cm^{-1}; II, $Dq = 1641$, $B_{35} = 647$, $B_{55} = 730$, $C = 2815$ cm^{-1}. These Dq values are slightly below average compared to octahedral Cr(III) in other oxygen-based structures, a tendency that was already observed for other $3d$ transition elements in crystal fields of selenite compounds. This might indicate a rather low position of the $[SeO_3]^{2-}$ anion within the range of oxygen-based ligands in the spectrochemical series. © 1998 Academic Press

[1] To whom correspondence should be addressed. E-mail: manfred.wildner@univie.ac.at.

INTRODUCTION

In the past few years, the crystal chemistry and hence the structural characterization of selenite compounds have gained increasing interest, especially due to the stereochemical consequences of the presence of the lone-pair electrons of the Se(IV) atoms; for a survey, cf. ref 1. The majority of these investigations deal with selenites of divalent transition metal ions. Among trivalent transition ions, particularly many Fe(III) selenites have been studied; a recent summary is given in ref 2. In spite of the fact that polyhedra of Fe(III) and Cr(III) exhibit similar average Me–O bond lengths (3), only two Cr(III) selenites have been structurally investigated up to now, namely, $Cr_2(SeO_3)_3 \cdot 3H_2O$ (4) and $Cr_2(Se_2O_5)_3$ (5), which both are isotypic with the respective iron selenites (5, 6). The present paper reports the structural and spectroscopic characterization of two polymorphs of the new compound $Cr(SeO_2OH)(Se_2O_5)$. Modification I is isotypic with the corresponding compounds of Fe(III) (7) and Mn(III) (8), while modification II represents a new structure type. In their paper on $Cr_2(Se_2O_5)_3$, Lafront *et al.* (5) pointed out that Bertaud (cf. ref 5), who reported different lattice constants for "$Cr_2(Se_2O_5)_3$," in fact studied the compound $Cr(SeO_2OH)(Se_2O_5)$-I. Transforming Bertaud's lattice constants to the $P2_1/n$ cell setting used here and in ref 8 and comparing them with the values listed in Table 1, this might indeed be the case (Bertaud's transformed cell: $a =$ 7.594 Å, $b = 12.553$ Å, $c = 7.356$ Å, $\beta = 90.95°$).

In addition, it seemed worthwhile to investigate the spectroscopic properties of the title compounds for several reasons. For instance, the electronic absorption spectra of transition metal selenites measured so far (9–12) indicate a rather low position of the $[SeO_3]^{2-}$ anion within the range of oxygen-based ligands in the spectrochemical series. This tendency is substantiated by the present UV–VIS absorption measurements. As a further aspect, hydroxyl groups of acid selenites usually form strong or very strong hydrogen bonds, leading to so-called AB or ABC bands in infrared spectra (13, 14). While a typical AB-band IR

TABLE 1

Crystal Data and Details of the X-Ray Data Collections and Structure Refinements of Two Modifications of Cr(SeO$_2$OH) (Se$_2$O$_5$)

	Cr(SeO$_2$OH)(Se$_2$O$_5$)-I	Cr(SeO$_2$OH)(Se$_2$O$_5$)-II
M_r	417.88	417.88
Space group	$P2_1/n$ (No. 14, cell choice 2)	$Pnma$ (No. 62)
a (Å)	7.517(2)	8.782(2)
b (Å)	12.516(3)	11.172(3)
c (Å)	7.381(2)	7.545(2)
β (°)	91.46(1)	
V (Å^3)	694.2	740.3
Z	4	4
ρ_{calc} (g cm^{-3})	3.998	3.750
μ(MoKα) (cm^{-1})	173.8	163.0
Crystal size (mm)	$0.15 \times 0.08 \times 0.05$	$0.10 \times 0.07 \times 0.06$
Crystal shape	(010) plate, elongated//a	forms {010}, {101}
Measured reflections	5375	3025
Unique data set	2519	1407
Variables	114	65
Transmission factors (ψ scans)	0.21–0.33	0.35–0.43
Extinction coefficient	0.00155	0.00112
R_{int}	0.059	0.065
w$R2$ (for all F_o^2)	0.065	0.056
$R1$ [for 1562, 752 $F_o > 4\sigma(F_o)$]	0.030	0.031
Goodness of fit	0.88	0.84
$(\Delta/\sigma)_{max}$	$< 10^{-3}$	$< 10^{-3}$
$\Delta\rho_{min/max}$ (e Å^{-3})	$-1.27/0.82$	$-1.21/1.05$

Note: $R1 = \sum ||F_o| - |F_c||/\sum |F_o|$;
w$R2 = [\sum w(F_o^2 - F_c^2)^2/\sum wF_o^4]^{1/2}$;
$w_{phase\ I} = 1/[\sigma^2(F_o^2) + (0.0255P)^2]$, $P = \{[\max(0\ or\ F_o^2)] + 2F_c^2\}/3$;
$w_{phase\ II} = 1/\sigma^2(F_o^2)$.

spectrum is observed for Cr(SeO$_2$OH)(Se$_2$O$_5$)-I, modification II exhibits uncommonly weak hydrogen bonding and thus provides new data for a correlation of IR spectroscopic data with structural data in acid selenites. For a short preliminary note on Cr(SeO$_2$OH)(Se$_2$O$_5$)-I, cf. ref 15.

EXPERIMENTAL

Emerald green single crystals of two modifications of Cr(SeO$_2$OH)(Se$_2$O$_5$) in sizes up to 0.2 mm were synthesized in a Teflon-lined steel vessel, starting with an appropriate mixture of Cr(OH)$_3$ and SeO$_2$ in H$_2$O. The closed vessel was kept at 220°C for 5 days and then cooled to room temperature within 12 h. In addition to crystals of the monoclinic phase I, only a few single crystals of the orthorhombic phase II ($\ll$ 1 vol%) were obtained. Single-crystal X-ray diffraction intensities up to $2\theta = 65°$ and 35 accurate 2θ values in the range 28°–34° for the least-squares refinement of lattice parameters were measured on a Stoe AED2 four-circle diffractometer using graphite-monochromatized MoKα radiation (293 K; 2θ–ω scans, 36 steps per reflection, increased for α_1–α_2 splitting, 2×5 steps for background correction; 0.03° and 0.5–2.0 s per step; three standard reflections every 60 min). The intensity data were corrected for Lorentz, polarization, and absorption effects (by ψ scans).

TABLE 2

Atomic Coordinates and Equivalent Displacement Parameters (Å^2) of Cr(SeO$_2$OH)(Se$_2$O$_5$)-I

	x	y	z	U_{eq}
Cr	0.44446(9)	0.67788(6)	0.31590(8)	0.0130(2)
Se1	0.05649(5)	0.80235(4)	0.39961(5)	0.0126(1)
Se2	0.07525(6)	0.63221(4)	0.08031(5)	0.0124(1)
Se3	0.73141(5)	0.51015(4)	0.43266(5)	0.0125(1)
O1	0.5309(4)	0.7563(3)	0.1020(4)	0.0154(6)
O2	0.2742(4)	0.7950(3)	0.3608(4)	0.0186(6)
O3	0.2739(4)	0.5933(3)	0.1669(4)	0.0176(7)
O4	0.6270(4)	0.7589(3)	0.4632(4)	0.0158(6)
O5	0.8792(4)	0.0668(3)	0.2420(4)	0.0156(6)
O6	0.6117(4)	0.3970(3)	0.4587(4)	0.0167(6)
O7	0.5959(5)	0.9565(3)	0.1951(5)	0.0240(8)
O8	0.5247(4)	0.1875(3)	0.2231(4)	0.0200(7)
H	0.579(10)	0.909(6)	0.145(10)	0.057(26)

The structure of phase I was refined on F^2 with the program SHELXL-93 (16), starting with the positional parameters given by Koskenlinna and Valkonen (8) for the non-hydrogen atoms in the isotypic compound Mn(SeO$_2$OH) (Se$_2$O$_5$). The position of the hydrogen atom was extracted from a difference Fourier map and refined isotropically. The structure of phase II was solved using direct methods (17) and subsequent Fourier and difference Fourier syntheses. In the refinement on F^2 (16), the O5–H distance was soft-restrained to 0.90(5) Å using SHELXL's DFIX instruction. Crystal data and details of the structure refinements for both modifications of Cr(SeO$_2$OH)(Se$_2$O$_5$) are summarized in Table 1; Tables 2 and 3 list final positional and equivalent displacement parameters. F_o–F_c tables and a table of anisotropic displacement parameters can be obtained from the corresponding author (M.W.) upon request.

Polarized electronic absorption spectra of Cr(SeO$_2$OH) (Se$_2$O$_5$)-I and -II in the range 33,000–12,500 cm^{-1} were measured at room temperature on a Zeiss UMSP-80

TABLE 3

Atomic Coordinates and Equivalent Displacement Parameters (Å^2) of Cr(SeO$_2$OH)(Se$_2$O$_5$)-II

	x	y	z	U_{eq}
Cr	0	1/2	0	0.0102(2)
Se1	0.28153(4)	0.39256(3)	0.20568(5)	0.0126(1)
Se2	0.98936(7)	1/4	0.79941(9)	0.0138(1)
O1	0.1202(3)	0.4696(2)	0.2151(4)	0.0170(6)
O2	0.3361(3)	0.3945(3)	0.4183(4)	0.0166(6)
O3	0.1878(5)	1/4	0.2133(7)	0.0180(9)
O4	0.0959(3)	0.3664(2)	0.8682(4)	0.0147(6)
O5	0.5323(7)	1/4	0.9279(7)	0.0324(14)
H	0.624(5)	1/4	0.934(9)	0.013(19)

microscope spectrometer. Spectral bandwidths and steps widths were both 1 nm, and the measuring spot was 40 μm in diameter. Details of the microscope spectrometric techniques are described in ref 18.

For monoclinic $Cr(SeO_2OH)(Se_2O_5)$-I, the following orientation of the axes of the optical indicatrix (arbitrarily labeled X, Y, Z) to the positive crystallographic axes is observed (with white light): $\measuredangle X, a = 22.5(5)°$, $\measuredangle X, c = 69.0(5)°$, $Y = b$, $Z \perp X, Y$. Spectra with the electric light vector parallel to X and Z were measured on the (010) face of a well-developed single crystal. Furthermore, a crystal slab polished parallel to (001) was prepared in analogy to previous papers (e.g. ref 9), enabling the measurement of the Y spectrum and of a spectrum parallel to the crystallographic a axis. As expected, the latter spectrum resembles the X spectrum and is ignored in this paper. The sample thicknesses were measured with a micrometer screw (polished sample: 20 ± 1 μm) or estimated by comparison with a micrometer scale (single crystal: 55 ± 5 μm). For orthorhombic $Cr(SeO_2OH)(Se_2O_5)$-II, optical indicatrix and crystallographic axes are arbitrarily correlated as follows: $X \parallel a$, $Y \parallel b$, $Z \parallel c$. X- and Z-polarized spectra were measured on the (010) face (estimated thickness: 55 ± 5 μm), the Y spectrum and a spectrum parallel to [101] were measured on the (10$\bar{1}$) face (estimated thickness: 70 ± 5 μm) of the same single crystal that was already used for the X-ray investigations.

Crystal field calculations were done using the Crystal Field Computer Package of Yeung and Rudowicz (19).

Single-crystal FTIR spectra were recorded in the region 7000–1000 cm^{-1} with Perkin-Elmer 1760X (phases I and II) and Bruker IFS66 spectrometers (phase II), both equipped with a FTIR microscope with a liquid N_2 cooled MCT detector. In the same spectral region, spectra of powdered samples of phase I diluted in KBr pellets were obtained with the 1760X spectrometer using a beam condensor with CsI lenses and a TGS detector.

RESULTS AND DISCUSSION

Crystal Structures

The crystal structures of the two modifications of $Cr(SeO_2OH)(Se_2O_5)$ are shown in Figs. 1 (phase I, projection along a) and 2 (phase II, projection along c); selected interatomic distances and bond angles are listed in Tables 4 and 5, respectively.

The structure of monoclinic $Cr(SeO_2OH)(Se_2O_5)$-I is isotypic with the corresponding compounds of Mn(III) (8) and Fe(III) (7). In this structure type isolated CrO_6 octahedra are connected by Se_2O_5 groups to corrugated sheets parallel to (010); each Se_2O_5 group (built up from Se1 and Se2) shares its four terminal oxygen corners with three CrO_6 octahedra. These sheets are interconnected by SeO_2OH groups (Se3)—linking two octahedra each—and their rather strong hydrogen bonds. The orthorhombic modification $Cr(SeO_2OH)(Se_2O_5)$-II represents a new structure type where isolated CrO_6 octahedra are linked via Se_2O_5 and SeO_2OH groups to a three-dimensional framework
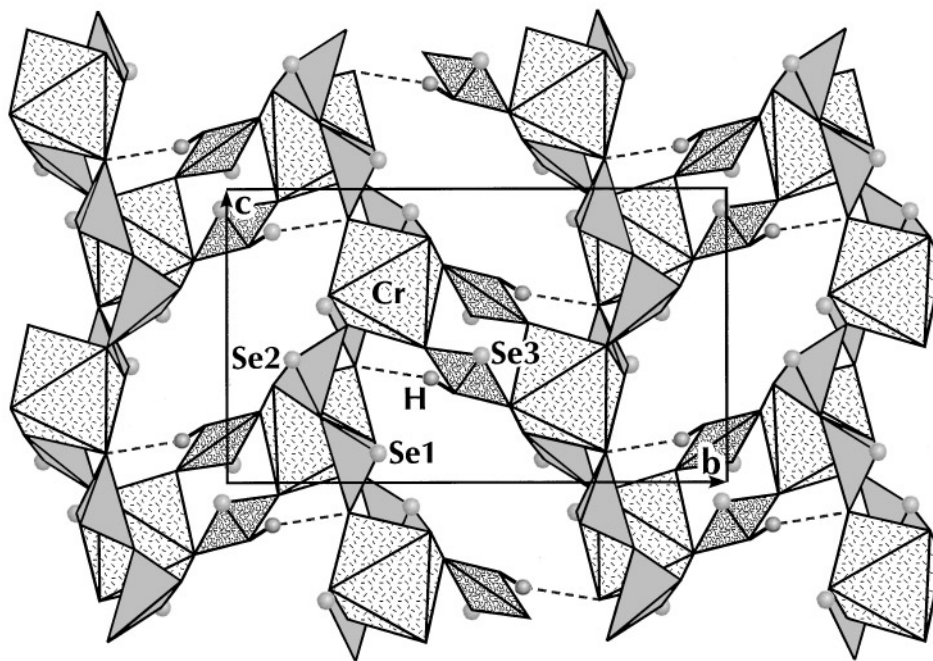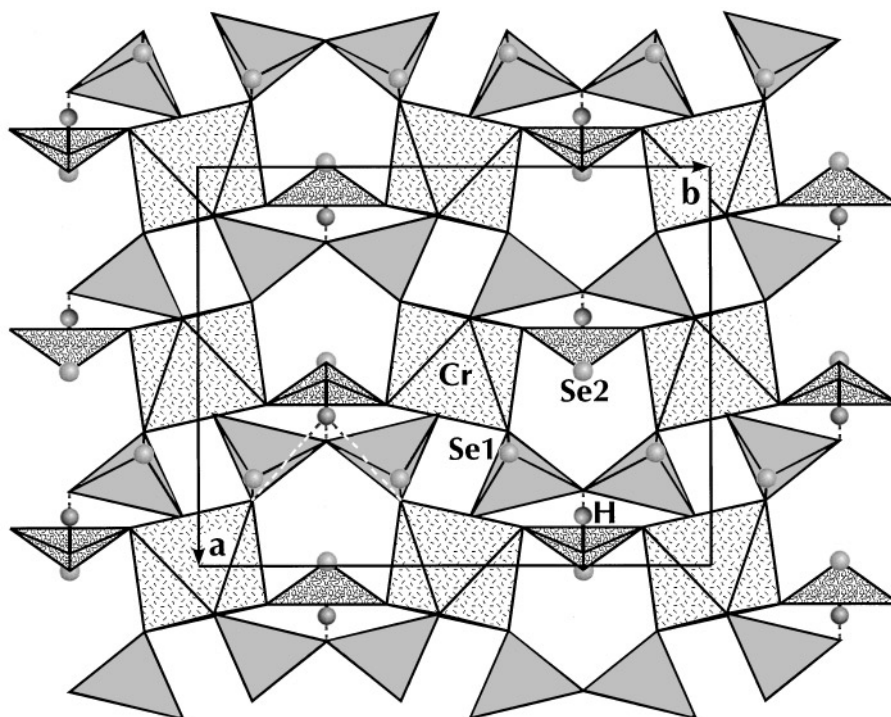

FIG. 1. Crystal structure of $Cr(SeO_2OH)(Se_2O_5)$-I in a projection along [100].

FIG. 2. Crystal structure of Cr(SeO$_2$OH)(Se$_2$O$_5$)-II in a projection along [001]. For one hydrogen atom, a possible bifurcation of the hydrogen bridge is indicated.

structure; here, the diselenite groups (built up from two Se1) each connect four CrO$_6$ octahedra by common corners, while each SeO$_2$OH group (Se2) again links two octahedra. The hydrogen bonds donated by the SeO$_2$OH groups are very weak and therefore play a minor role in the structure of phase II.

In both compounds, the CrO$_6$ polyhedra exhibit nearly regular octahedral shapes and mean Cr(III)–O bond lengths in agreement with crystal chemical expectations. For example, in two further Cr(III) selenites that have been structurally characterized so far, Cr$_2$(SeO$_3$)$_3$ · 3H$_2$O (4) and Cr$_2$(Se$_2$O$_5$)$_3$ (5), $\langle$Cr(III)–O$\rangle$ distances range from 1.965 to 1.990 Å. In Cr(SeO$_2$OH)(Se$_2$O$_5$)-I the mean bond length and the bond length distortion are slightly higher compared to II. Nevertheless, the type of this distortion cannot be correlated with the strong [4+2] Jahn–Teller elongation of the Mn(III) O$_6$ polyhedron in the isotypic manganese compound (8); actually, the axis of elongation in the MnO$_6$ polyhedron, O1–O6, represents the shortest axis of the CrO$_6$ octahedron in phase I.

The Se(IV) atoms are characteristically one-sided pyramidally coordinated to three oxygen atoms, a consequence of the activity of the lone-pair electrons of tetravalent selenium atoms. The SeO$_2$OH as well as the Se$_2$O$_5$ groups have usual mean Se–O distances and exhibit typical bond length distortions with Se–OH and bridging Se–O bond lengths close to corresponding average values given in the

literature, i.e., 1.761 Å for Se–OH bonds of SeO$_2$OH groups (average mean Se–O = 1.702 Å) and 1.818 Å for Se–O bridges of Se$_2$O$_5$ groups (average mean Se–O = 1.717 Å) (1). The Se–O–Se angles of the diselenite groups, $\sim$125° in both compounds, are comparatively large: Se–O–Se angles of 29 Se$_2$O$_5$ groups found in 21 diselenite compounds (out of 24 diselenites described so far in the literature) range from 115.3° in Au$_2$(SeO$_3$)$_2$(Se$_2$O$_5$) (20) to 126.4° in the Mn analog of phase I, Mn(SeO$_2$OH)(Se$_2$O$_5$) (8). The only exceptions are the isotypic compounds MnSe$_2$O$_5$ (21) and CdSe$_2$O$_5$ (22), with Se–O–Se angles of 136.9° and 140.3°, respectively. These values are classified by the respective authors as "inexplicable" (21) and "typical of diselenites" (22) (the latter is obviously not the case). For Ca$_2$(SeO$_2$OH)$_2$(Se$_2$O$_5$) (23) a Se–O–Se angle of 131.3° is given assuming a special, twofold position for the bridging oxygen. However, according to the structure refinement, the position of this oxygen atom is split around the twofold axis, resulting in a 'normal' Se–O–Se angle of 122.3°. Evidently, a lot more structural data on new diselenite compounds are required for a thorough stereochemical discussion on Se–O–Se angles of Se$_2$O$_5$ groups.

Hydrogen Bonding and Related IR Spectroscopic Data

The hydrogen-bonding system in Cr(SeO$_2$OH)(Se$_2$O$_5$)-I is clear-cut (Table 4 and Fig. 1) and corresponds to the

TABLE 4
Selected Interatomic Distances (Å) and Bond Angles (Deg)
in Cr(SeO$_2$OH)(Se$_2$O$_5$)-I

Cr octahedron			
Cr–O1	1.983(3)	O1–Cr–O2	89.6(1)
–O2	1.980(3)	–O3	92.5(1)
–O3	1.975(3)	–O4	87.0(1)
–O4	2.004(3)	–O5	86.6(1)
–O5	1.975(3)	–O6	172.9(1)
–O6	1.964(3)	O2–Cr–O3	94.4(1)
⟨Cr–O⟩	1.980	–O4	88.3(1)
		–O5	176.2(1)
		–O6	93.3(1)
Hydrogen bond		O3–Cr–O4	177.2(1)
O7–H	0.71(7)	–O5	86.1(1)
H···O1	1.97(7)	–O6	93.8(1)
O7–O1	2.640(5)	O4–Cr–O5	91.1(1)
O7–H···O1	158(8)	–O6	86.6(1)
		O5–Cr–O6	90.4(1)
Se environments			
Se1–O1	1.680(3)	O1–Se1–O2	105.3(2)
–O2	1.671(3)	–O8	93.1(1)
–O8	1.797(3)	O2–Se1–O8	101.0(1)
⟨Se1–O⟩	1.716	⟨O–Se1–O⟩	99.8
Se2–O3	1.682(3)	O3–Se2–O4	102.6(1)
–O4	1.665(3)	–O8	101.0(1)
–O8	1.790(3)	O4–Se2–O8	102.3(1)
⟨Se2–O⟩	1.712	⟨O–Se2–O⟩	101.9
	Se1–O8–Se2	125.0(2)	
Se3–O5	1.674(3)	O5–Se3–O6	100.8(1)
–O6	1.692(3)	–O7	96.2(2)
–O7	1.757(4)	O6–Se3–O7	98.2(2)
⟨Se3–O⟩	1.708	⟨O–Se3–O⟩	98.4

TABLE 5
Selected Interatomic Distances (Å) and Bond Angles (Deg)
in Cr(SeO$_2$OH)(Se$_2$O$_5$)-II

Cr octahedron					
Cr–O1	2 ×	1.965(3)	O1–Cr–O2	2 ×	88.2(1)
–O2	2 ×	1.960(3)	–O2	2 ×	91.8(1)
–O4	2 ×	1.981(3)	–O4	2 ×	86.8(1)
⟨Cr–O⟩		1.969	–O4	2 ×	93.2(1)
			O2–Cr–O4	2 ×	89.0(1)
			–O4	2 ×	91.0(1)
Possible hydrogen bonds					
O5–H		0.81(4)			
H···O3		2.72(7)	H···O2	2 ×	2.70(4)
O5–O3		3.032(7)	O5–O2	2 ×	3.327(6)
O5–H···O3		105(5)	O5–H···O2	2 ×	135(3)
Se environments					
Se1–O1		1.660(3)	O1–Se1–O2		101.4(2)
–O2		1.674(3)	–O3		93.9(2)
–O3		1.794(3)	O2–Se1–O3		96.4(2)
⟨Se1–O⟩		1.709	⟨O–Se1–O⟩		97.2
	Se1–O3–Se1	125.2(2)			
Se2–O4	2 ×	1.684(3)	O4–Se2–O4		101.1(1)
–O5		1.756(5)	–O5	2 ×	100.5(2)
⟨Se2–O⟩		1.708	⟨O–Se2–O⟩		100.7

model proposed for the isotypic iron compound (7), where the hydrogen atom could not be located [for the isotypic Mn compound (8) neither a H position nor a hydrogen-bonding scheme was proposed]. The SeO$_2$OH group donates a rather strong hydrogen bond with an O7–H···O1 distance of 2.640 Å. The infrared spectrum exhibits an AB-band system due to Fermi resonance of the ν_{OH} stretching mode with the 2δ_{OH} in-plane bending overtone, as typically observed also for acid selenites of divalent metals (13, 14). IR absorption bands related to hydrogen bonding are observed at 1248 (δ_{OH} in-plane bending mode), 2425 (2δ_{OH} overtone, B band), 2890 (ν_{OH} stretching mode, A band), and ~4200 cm^{-1} [$\nu_{OH}(A) + \delta_{OH}$ combination mode]. In the isotypic Fe(III) compound (7), where O–H···O is 2.670 Å, the AB bands and δ_{OH} are reported at 2853, 2395, and 1233 cm^{-1}, respectively. Both data sets agree reasonably well with those observed for various acid M(II) selenites containing comparable O–H···O distances (13, 14) as well as with general correlations found for ν_{OH} stretching frequencies versus O–H···O bond lengths (e.g., refs 24 and 25).

It is worth mentioning that in Cr(SeO$_2$OH)(Se$_2$O$_5$)-I a further interpolyhderal O···O contact (cf. 26) shorter than 3.0 Å occurs, O7···O8 = 2.949 Å, which is obviously not involved in the hydrogen-bonding system of this compound.

Contrary to the strong hydrogen bonds most commonly found in acid selenites (13, 14), possible hydrogen bonds in Cr(SeO$_2$OH)(Se$_2$O$_5$)-II, donated by oxygen O5, are very weak. A single bridge, O5–H···O3, located in the mirror plane, has O···O = 3.032 Å, while the position of the H atom (which is, of course, not very reliable when determined by X-ray diffraction) favors a bifurcation to O2 with O5–H···O2 = 3.327 Å. The assignment of the IR spectrum is not as straightforward as for phase I, and unfortunately, there are hardly any correlation data for very weak or bifurcated bonds in the literature. In any case, a discussion in terms of an AB-band system seems not appropriate, since Fermi resonances are expected to be negligible. Bands at 1050 or 1315 cm^{-1} might represent the δ_{OH} bending mode. The ν_{OH} stretching band is split up with maxima at 3385 and 3435 cm^{-1}, and a much weaker component occurs at 3655 cm^{-1}; the 2ν_{OH} overtone at 6690 cm^{-1} is not split up. A very sharp band at 4461 cm^{-1} can be assigned to the $\nu_{OH} + \delta_{OH}$ combination mode; this indicates that the band at 1050 cm^{-1} is δ_{OH}, and a further sharp band at 2083 cm^{-1} represents its practically unperturbed overtone 2δ_{OH}. However, the rather strong intensity of the latter band in single-crystal spectra is in contradiction to its large frequency separation from the stretching mode ν_{OH}.
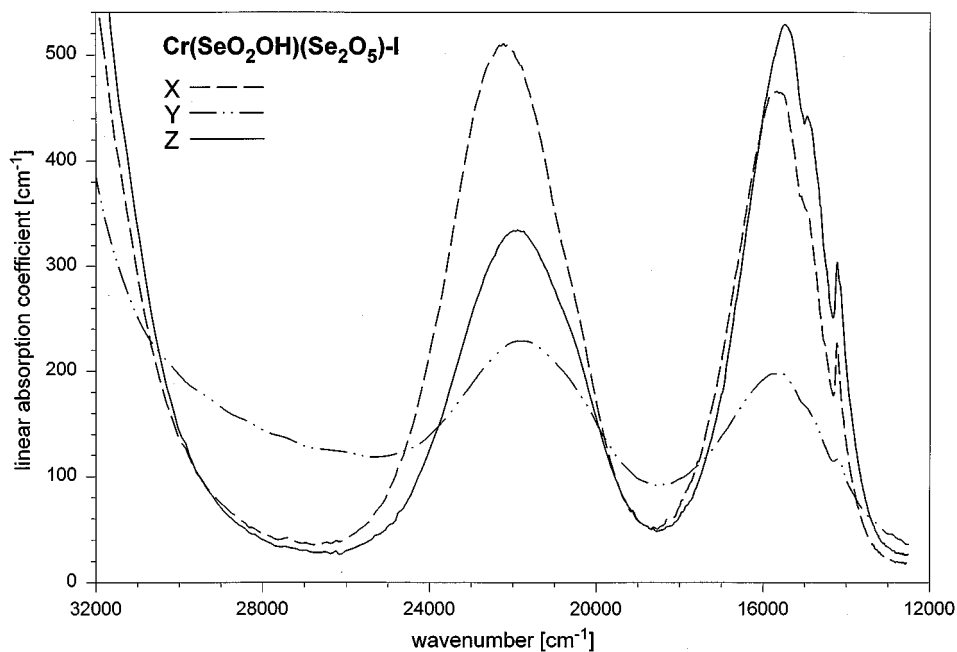
FIG. 3. Polarized absorption spectra of Cr(SeO$_2$OH)(Se$_2$O$_5$)-I in the region 12,500–32,000 cm^{-1}.

Electronic Absorption Spectra

Polarized electronic absorption spectra of Cr(SeO$_2$OH)(Se$_2$O$_5$)-I and -II are presented in Figs. 3 and 4, respectively. Observed band positions, assignments, and results of crystal field calculations (assuming O_h symmetry) are summarized in Table 6. The spectra are characterized by two intense absorption bands in the visible region, which are typical of Cr(III) ions in octahedral coordination by oxygen atoms. These bands, in the title compounds located around 16,000 and 22,500 cm^{-1} with typical bandwidths at half-height of ~ 2500 and ~ 3200 cm^{-1}, can be assigned to the

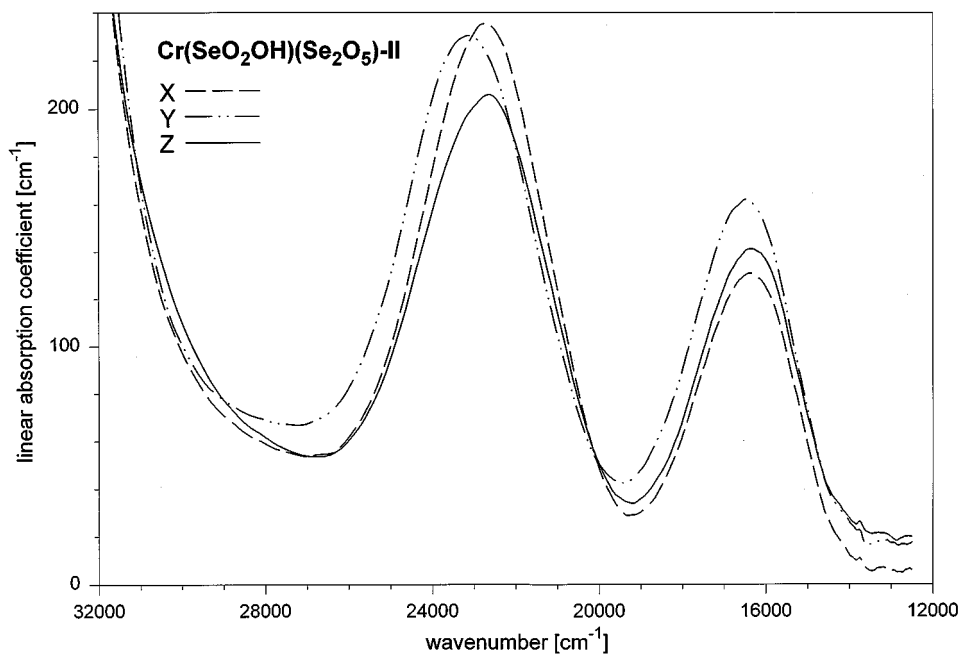**FIG. 4.** Polarized absorption spectra of Cr(SeO$_2$OH)(Se$_2$O$_5$)-II in the region 12,500–32,000 cm^{-1}.

<div align="center">

TABLE 6

Crystal Field Parameters (cm^{-1}), Observed and Calculated Energy Levels (cm^{-1}), and Corresponding O_h Assignments
(with Parental Free-Ion Terms in Parentheses) for Two Modifications of Cr(SeO$_2$OH)(Se$_2$O$_5$)

</div>

Cr(SeO$_2$OH)(Se$_2$O$_5$)-I ($Dq = 1558$, $B_{35} = 653$, $B_{55} = 760$, $C = 2920$)		Cr(SeO$_2$OH)(Se$_2$O$_5$)-II ($Dq = 1641$, $B_{35} = 647$, $B_{55} = 730$, $C = 2815$)		
Observed	Calculated	Observed	Calculated	Assignment
	0		0	$^4A_{2g}(^4F)$
14,225	14,228	13,750	13,750	$^2E_g(^2G)$
14,948	14,951	—	14,434	$^2T_{1g}(^2G)$
~15,490 (Z), ~15,670 (XY)	15,580	~16,370 (XZ), ~16,450 (Y)	16,410	$^4T_{2g}(^4F)$
~20,280 (XY), ~20,400 (Z)	21,213	—	20,692	$^2T_{2g}(^2G)$
~21,840 (YZ), ~22,220 (X)	22,030	~22,700 (XZ), ~23,100 (Y)	22,900	$^4T_{1g}(^4F)$
—	~27,000–34,000	—	~27,500–34,500	(^2G, ^2H, ^2P)
—	34,502	—	36,029	$^4T_{1g}(^4P)$

spin-allowed $^4A_{2g}(F) \rightarrow {}^4T_{2g}(F)$ and $^4A_{2g}(F) \rightarrow {}^4T_{1g}(F)$ transitions. The third spin-allowed transition to the $^4T_{1g}(P)$ level, expected above 34,000 cm^{-1}, is obscured by the charge transfer absorption edges at ~32,000 cm^{-1}. In the spectra of phase I, a few spin-forbidden quartet → doublet transitions are clearly observed: sharp peaks at 14,225 and 14,948 cm^{-1} are attributed to the nearly field-independent $^2E_g(G)$ and $^2T_{1g}(G)$ levels, both derived from the t_{2g}^3 electron configuration. A weak shoulder (~20,340 cm^{-1}) at the low-energy wing of the intense $^4T_{1g}(F)$ band might be correlated with the transition to $^2T_{2g}(G)$; this level also belongs to the t_{2g}^3 configuration but has a somewhat stronger dependence from the crystal field strength Dq compared to $^2E_g(G)$ and $^2T_{1g}(G)$. This may explain the bandwidth of ~700 cm^{-1} (FWHH, derived from Gaussian peak fitting analysis) in room temperature spectra. In phase II, only one weak band, at 13,750 cm^{-1}, can be ascribed to a spin-forbidden transition, i.e., to the $^2E_g(G)$ level. Spectral features at lower wavenumbers are obviously caused by background noise.

The different magnitude of the absorption intensity in the d–d spectra of the title compounds is correlated to the extent of violation of the Laporte selection rule within the CrO$_6$ octahedra, in phase I (Cr site symmetry 1) realized by the static absence of a center of symmetry, and in phase II (Cr site symmetry $\bar{1}$) only by dynamic removal due to uneven octahedral vibrations. As a consequence of the comparatively weak octahedral distortions—leading to rather small band splittings and polarization effects (especially in phase II)—no obvious higher polyhedral pseudosymmetry can be proposed for a detailed analysis of level splittings and symmetry selection rules. Thus, crystal field calculations were performed assuming O_h symmetry for the Cr(III)O$_6$ octahedra in both compounds.

For a d^3 electron configuration in octahedral fields, the first spin-allowed transition $^4A_{2g}(F) \rightarrow {}^4T_{2g}(F)$ equals $10Dq$; i.e., Dq is 1558 cm^{-1} in phase I and 1641 cm^{-1} in phase II.

On the one hand, this difference in the crystal field strength correlates with the sequence of the mean Cr–O bond lengths; on the other hand, it is surprisingly large considering that the ⟨Cr–O⟩ distances differ by only 0.011 Å. Generally, the observed Dq values are slightly below average compared with data for Cr(III) in other oxygen-based structures, e.g., in minerals, where Dq mostly ranges between ~1550 and ~1850 cm^{-1} (27), or with $Dq = 1740$ cm^{-1} for Cr(III) in aqueous solution (28). A similar tendency was also found for other $3d$ transition elements in crystal fields of selenite compounds investigated so far, i.e., Mn(IV) (10) and Co(II) (9, 11, 12), thus indicating a rather low position of the [SeO$_3$]$^{2-}$ anion within the range of oxygen-based ligands in the spectrochemical series. The Racah parameters B_{35} —evaluated from Dq and the second spin-allowed transition, $^4A_{2g}(F) \rightarrow {}^4T_{1g}(F)$—and the resulting nephelauxetic ratios β_{35} (relative to the free-ion value $B_0 = 918$ cm^{-1}) are practically equal in both compounds (I: $B_{35} = 653$ cm^{-1}, $\beta_{35} = 0.71$; II: $B_{35} = 647$ cm^{-1}, $\beta_{35} = 0.70$). These values are intermediate within the wide range of B_{35} values given in the literature for Cr(III) in fields of oxygen ligands. As expected, Racah B_{55}, relevant for forbidden spin-flip transitions within the t_{2g} orbitals, is significantly higher than B_{35}. In phase I, B_{55} and Racah C were fitted to the $^2E_g(G)$ and $^2T_{1g}(G)$ levels ($B_{55} = 760$ cm^{-1}, $\beta_{55} = 0.83$, $C = 2920$ cm^{-1}); in phase II, where only $^2E_g(G)$ is observed, the same C/B ratio as in phase I was assumed, leading to $B_{55} = 730$ cm^{-1} ($\beta_{55} = 0.80$) and $C = 2815$ cm^{-1}.

Additional crystal field calculations including spin–orbit coupling were performed to estimate the influence of "intensity stealing," i.e., the extent of admixture of quartet character to the spin-forbidden doublet states. The spin–orbit coupling constant ζ was set to 200 cm^{-1}. The results correspond very well with the observed intensities of the spin-forbidden transitions: In Cr(SeO$_2$OH)(Se$_2$O$_5$)-I, $^2E_g(G)$ and

$^2T_{1g}(G)$ both gain up to more than 2% quartet character, while $^2T_{2g}(G)$ gains about 1.2%. In contrast, in Cr(SeO$_2$OH) (Se$_2$O$_5$)-II, where $^2E_g(G)$ represents the only (weakly) observed spin-forbidden band, this level has $\sim$0.6% quartet admixture, while for $^2T_{1g}(G)$ and $^2T_{2g}(G)$ it is less than 0.3%.

REFERENCES

1. M. Koskenlinna, *An. Acad. Sci. Fenn.-Chem.* **262,** 1 (1996). [Thesis, Helsinki University of Technology]
2. G. Giester, *Z. Anorg. Allg. Chem.* **622,** 1788 (1996).
3. W. H. Baur, *in* "Structure and Bonding in Crystals" (M. O'Keeffe and A. Navrotsky, Eds.), Vol. II. p. 31. Academic Press, New York, 1981.
4. W. T. A. Harrison, G. D. Stucky and A. K. Cheetham, *Eur. J. Solid State Inorg. Chem.* **30,** 347 (1993).
5. A. M. Lafront, J. Bonvoisin and J. C. Trombe, *J. Solid State Chem.* **122,** 130 (1996).
6. G. Giester and F. Pertlik, *J. Alloys Compd.* **210,** 125 (1994).
7. H. Muilu and J. Valkonen, *Acta Chem. Scand., Ser. A* **41,** 183 (1987).
8. M. Koskenlinna and J. Valkonen, *Acta Chem. Scand., Ser. A* **31,** 638 (1977).
9. M. Wildner and K. Langer, *Phys. Chem. Miner.* **20,** 460 (1994).
10. M. Wildner and K. Langer, *Phys. Chem. Miner.* **21,** 294 (1994).
11. M. Wildner, *J. Solid State Chem.* **115,** 360 (1995).
12. M. Wildner, *J. Solid State Chem.* **124,** 143 (1996).
13. K. Unterderweide, B. Engelen, and K. Boldt, *J. Mol. Struct.* **322,** 233 (1994).
14. K. Unterderweide, Thesis, University of Siegen, Germany, 1995.
15. M. Wildner and M. Andrut, *Z. Kristallogr.* **11,** 95 (1996). [Suppl. Issue]
16. G. M. Sheldrick, "SHELXL-93: A Program for Crystal Structure Refinement," University of Göttingen, Germany, 1993.
17. G. M. Sheldrick, "SHELXS-86: A Program for the Solution of Crystal Structures," University of Göttingen, Germany, 1986.
18. K. Langer and K. R. Fentrup, *J. Microsc.* **116,** 311 (1979).
19. Y. Y. Yeung and C. Rudowicz, *Comput. Chem.* **16,** 207 (1992).
20. P. G. Jones, E. Schwarzmann, G. M. Sheldrick, and H. Timpe, *Z. Naturforsch. B: Chem. Sci.* **36,** 1050 (1981).
21. J. Bonvoisin, J. Galy, and J. C. Trombe, *J. Solid State Chem.* **107,** 171 (1993).
22. J. Valkonen, *Acta Crystallogr., Sect. C: Cryst. Struct. Commun.* **50,** 1381 (1994).
23. J. Valkonen, *J. Solid State Chem.* **65,** 363 (1986).
24. A. Novak, *Struct. Bonding* **18,** 177 (1974).
25. W. Mikenda, *J. Mol. Struct.* **147,** 1 (1986).
26. J. Zemann, *Z. Kristallogr.* **175,** 299 (1986).
27. R. G. Burns, "Mineralogical Applications of Crystal Field Theory," 2nd ed. Cambridge University Press, Cambridge, 1993.
28. C. K. Jørgensen, *Adv. Chem. Phys.* **5,** 33 (1963).